Seismic design of deep pier foundations in very soft clayey soils

V. Licata
Anas S.p.A., Rome, Italy

R. Conti
Università di Roma Niccolò Cusano, Rome, Italy

R. Di Laora
Università della Campania "Luigi Vanvitelli", Aversa, Italy

L. de Sanctis
Università di Napoli Parthenope, Naples, Italy

E. Mittiga, A. Micheli
Anas S.p.A., Rome, Italy

ABSTRACT: This paper presents the results of a numerical and theoretical study aimed at identifying optimal design solutions for the seismic design of bridge pier foundations in very soft soil deposits. The reference case study consists of the pier foundations of a cross-river bridge designed to complete a highway over the Po Valley (Northern Italy). The subsoil is of sedimentary origin, with alternating layers of clayey silts and clays interbedded by thin layers of silty sand and peat. The mechanical properties of the soils were defined by conventional site and laboratory investigations, including Resonant Column tests carried out to define the dissipative and nonlinear behaviour of the soils. Numerical 2D and 3D models are used to assess the dynamic soil-structure interaction for the bridge piers, focusing both on inertial and kinematic effects. The main goal of the work is to highlight the influence of the type and layout of the foundation system on the overall seismic response of the bridge pier.

1 INTRODUCTION

Pile and shaft/caisson foundations, usually adopted to support bridge piers in soft soil deposits, are characterized by different load transfer mechanisms, which essentially rely on the lateral soil shear stresses in the first case, while including also the soil normal stresses at the base in the second case. This main difference, which affects the overall behaviour and design of the foundation under both static (essentially vertical) and seismic loads, stems from the different depth-to-width ratio, which is typically in the range of 0.5 - 4 for shaft/caisson foundations and larger than 8 for piles.

The seismic design of bridge piers is usually carried out under a fixed-base assumption, that is neglecting any possible interaction between the deck-pier system and the underlying soil-foundation system. This approach usually leads to an over-estimation of the seismic demand in the bridge and, then, to an over-design of both the structure and the foundation.

As a matter of fact, soil-structure interaction (SSI) can modify the dynamic response of a structure, with respect to its rigidly supported counterpart, in at least three different ways: (1) by allowing dissipation of energy into the soil in the form of radiation and hysteretic damping, (2) by lengthening the fundamental period of the structure, and (3) by filtering the incident seismic wave field imposed at the base of the structure. The latter effect is typically relevant for embedded and deep foundations, where the horizontal motion of the foundation is reduced with respect to the free-field one, but a rotational component can emerge as a result of the interaction between the foundation and the soil (Conti *et al.*, 2017, 2018; Di Laora *et al.*, 2017). As a general trend, additional dissipation of energy always leads to a reduction of the structural response, while the other two effects can be either beneficial or detrimental, depending on the geometry of the structure and on resonance phenomena between the input earthquake and the system (Mylonakis & Gazetas, 2000).

From a conceptual point of view, SSI can be thought as the contribution of two concurrent phenomena: (i) a kinematic interaction, in which the foundation modifies the motion of the surrounding soil by means of its stiffness, and (ii) an inertial interaction, in which the motion of the foundation itself is further modified by the inertial forces acting in the structure. The distinction between kinematic and inertial effects turns out to be convenient also from a computational point of view, as it underlies the well-established substructure method.

This paper presents some of the results of a theoretical and numerical study aimed at identifying and quantifying SSI effects in bridge deck-pier-foundation systems. Specifically, the main differences in the dynamic response of a bridge pier founded on shaft and pile foundations are highlighted. The reference case study is given by the foundations of a cross-river bridge designed to complete a highway over the Po Valley (Northern Italy), corresponding to which a large amount of data from both site investigations and laboratory tests were available to characterize the subsoil deposit profile.

In the following sections, the structure and the geotechnical soil model are firstly defined, based on the available information and experimental data. Then, the main results of seismic site response analyses are presented. Finally, the dynamic interaction problem is investigated by means of numerical simulations carried out with the FEM code ANSYS.

2 STRUCTURE AND GEOTECHNICAL SOIL MODEL

2.1 *Physical and mechanical properties of the soils*

The geotechnical soil model was based on an accurate site investigation and laboratory campaign, which allowed acquiring a comprehensive frame of the buried setting and of the mechanical behavior of the soils. The campaign, executed along the progression of the road, consisted of approximately 30 boreholes, with the sampling of undisturbed and remolded specimens, Down Hole tests (DH), Nakamura test (HVSR), Resonant Columns tests (RC) and cone penetration tests (CPT). Figure 1 shows the geological reconstruction under the bridge, obtained from boreholes and the CPTs tests. It is essentially characterized by normally consolidated fine-grained soils spaced out by a deep silty sand layer and a shallow peat layer.

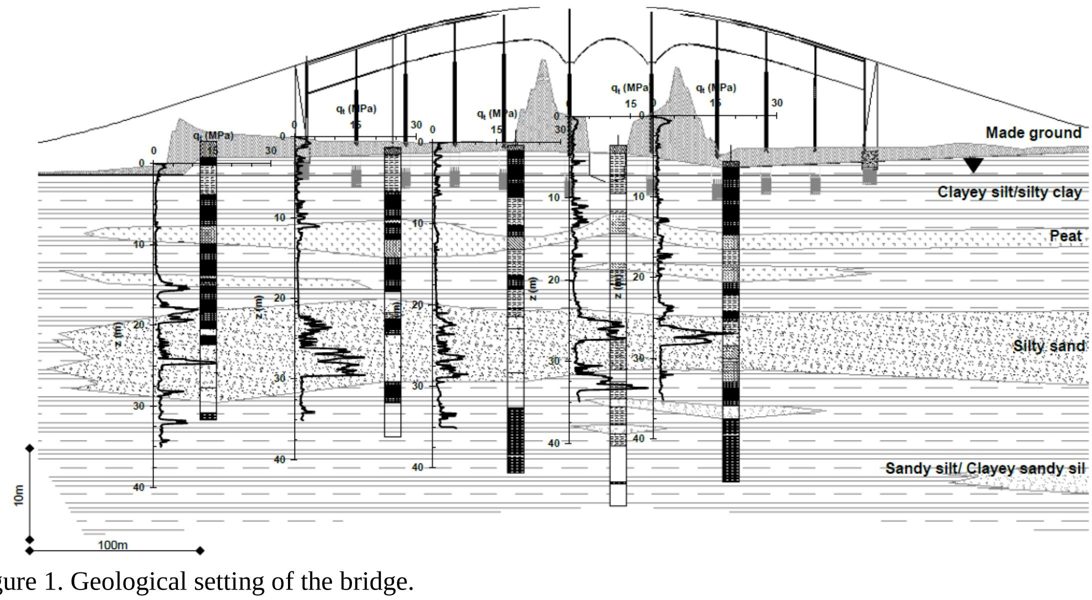

Figure 1. Geological setting of the bridge.

The grain size distributions of the materials is shown in Figure 2a. For comparison, Figures 2b-c report also the plasticity chart, the organic content (OC) and the unit weight (γ) of each lithotype. The shear wave velocity profiles were inferred from the results of the DH tests (Figure 2d). Finally, the dissipative and non-linear properties of the soils, in the form of the shear modulus degradation and damping curves, were assumed from the results of the RC tests for the clayey silt/silty clay and the peat and from the Darendeli (2001) empirical curves for the other materials (Figure 2e).

The assumed geotechnical model is synthetized in Table 1.

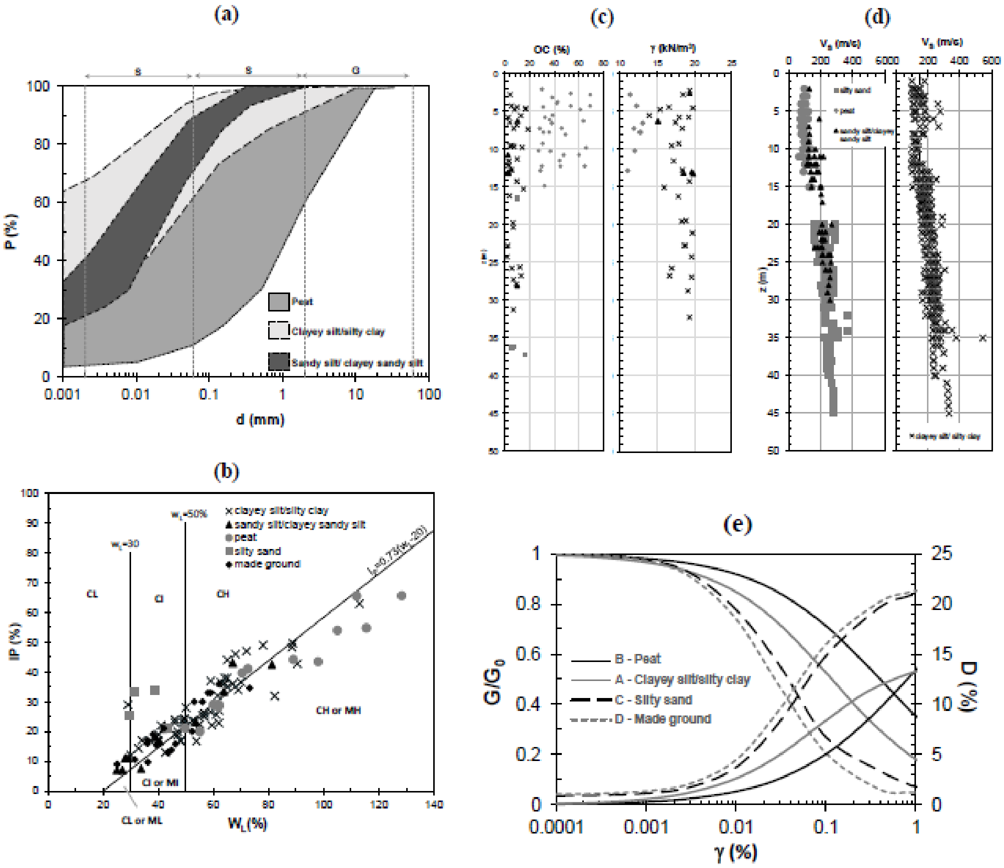

Figure 2. Results of laboratory test in terms of grain size distributions (a), plasticity chart (b), organic content and unit weight (c). V_S profiles (d) and dissipative and non-linear properties (e) for each lithotype.

Table 1. Geotechnical soil model.

Material	z	IP	γ	OCR	K_0	V_S	RCTS
	m	%	kN/m^3			m/s	
Made ground	0-5	10	18	1	0.61	125	D
Clayey silt /silty clay	5-14	30	16	1	0.66	130	A
Peat	14-16	50	12	1	0.53	97	B
Clayey silt /silty clay	16-20	30	16	1	0.66	170	A
	20-24	30	16	1	0.66	200	A
Silty sand	24-29	5	18	1	0.50	235	C
Clayey silt /silty clay	29-40	30	18	1	0.63	250	A
	40-60	30	18	1	0.63	350	A
	60-80	30	18	1	0.63	450	A
	90-100	30	18	1	0.63	500	A
Bedrock	>100	-	20	-	-	800	-

2.2 *Definition of the seismic bedrock*

The available results of the DH tests allowed investigating the subsoil up to 45 m depth. As shown in Figure 2d, the maximum V_S at the investigated depth is approximately 300 m/s and, thus, the seismic bedrock (characterized by V_S > 800 m/s) was not found. To overcome this drawback, the bedrock was defined by adopting the results of the available HVSR tests (shown in Figure 3). More in detail, 1D linear elastic analyses were performed varying the depth of the seismic bedrock, $z_{bedrock}$, as long as the analytical amplification curves matched the HVSR experimental amplification curve.

Figure 3 shows a comparison between the experimental amplification curves inferred from two HVSR tests (black dashed line) with the linear-elastic analytical curve, computed assuming $z_{bedrock}$=100m (black continuous line). The comparison shows a good match between the analytical and experimental frequencies of the 1st mode (≈1Hz), typically associated to the vibration of the entire deformable column above the top of the bedrock. Moreover, the analytical curve also fits the frequencies of the 2nd and 3rd experimental modes, thus, demonstrating the accuracy of the V_S model adopted in the seismic analyses.

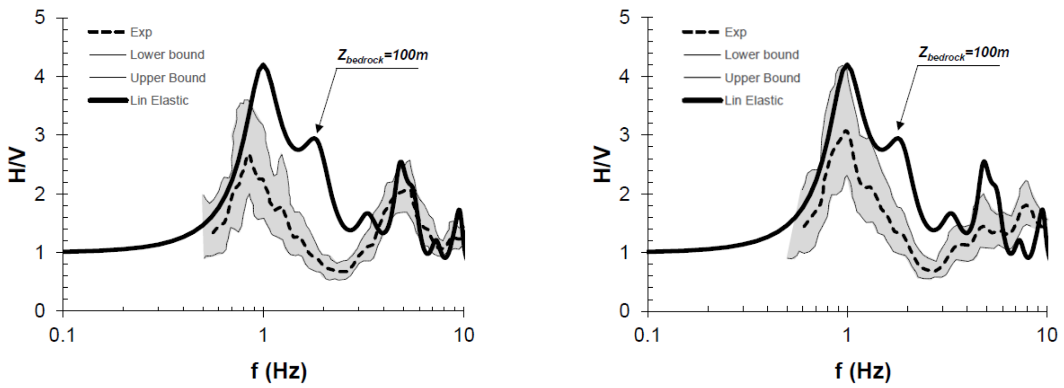

Figure 3. Comparison between linear-elastic amplification curve with two HVSR esperimental amplification curves, by assuming a depth of 100m as seismic bedrock.

2.3 *Bridge data*

The bridge is characterized by 10 spans with variable length, with an overall length of approximately 250m.

The results presented in this study refer to the two identical central piers of the bridge. Each pier consists in a single hammerhead reinforced concrete column of height H_{str} = 11 m and diameter d_{str} = 3.0 m. The total vertical load transferred by the deck is 16000 kN, while the weights of the pier cap and of the pier are 1400 kN and 1950 kN, respectively.

The top of the foundation is located 6 m below ground level. Two foundation types are considered in this work, both designed under static loads in order to guarantee an adequate margin of safety against the bearing capacity failure mechanism, *i.e.*:

1. a circular *shaft foundation*, with diameter d_{sh} = 8 m, embedment depth L_{sh} = 12 m, unit weight γ_{sh} = 20 kN/m^3.
2. a 3×3 *pile group* consisting of reinforced concrete piles with diameter d_p = 1 m and length L_p = 36 m. The piles are rigidly capped by a 2 m thick reinforced concrete raft.

Figure 4 shows a plan view of the two foundations.

3 SEISMIC SITE RESPONSE ANALYSES

3.1 *Input signals*

The input signals were selected to be compatible with the code-specified spectrum of the life-safety limit state, corresponding to an earthquake action with a 10% probability of exceedance during the life-span of the bridge and a return period of 950 years.

The code Rexel (Iervolino *et al.*, 2010) was used to select seven natural acceleration time histories, from Italian (ITACA) and European databases (ESM), recorded on outcropping rock (soil class A according to Eurocode 8) to limit the influence of site condition on duration, amplification and frequency range of the signals. Particularly, they were defined by a preliminary de-aggregation (partitioning) of the seismic hazard into selected magnitude (M) and distance (R), so as to identify the modal contribution to the overall site hazard. Figure 5 shows the elastic response spectra at 5% damping of the selected signals.

3.2 *Results of seismic site response analyses*

1D linear equivalent analyses were carried out to investigate the seismic response of the soil deposit under the design earthquakes. The main results are summarized in Figure 6 in terms of profiles of: (a) maximum acceleration, a_{max}; (b) maximum shear strain, γ_{max}; (c) mobilized shear wave velocity, V_S; and (d) damping ratio, D.

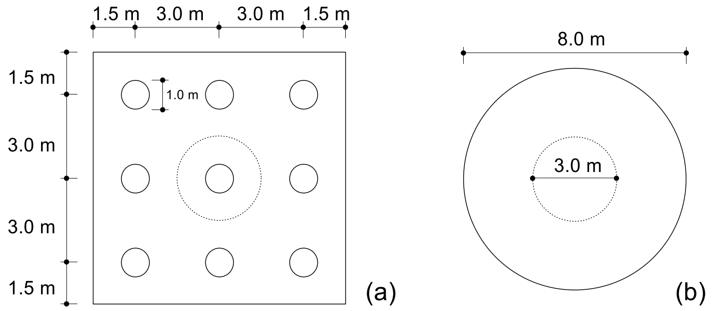

Figure 4. Plan view of the foundations: (a) pile group foundation and (b) circular shaft foundation.

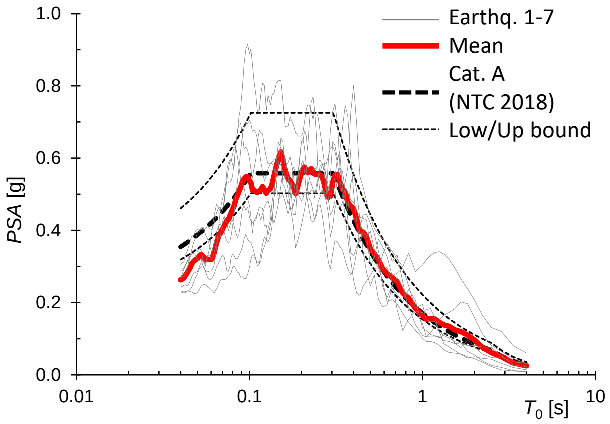

Figure 5. Elastic response spectra at 5% damping of the input earthquakes.

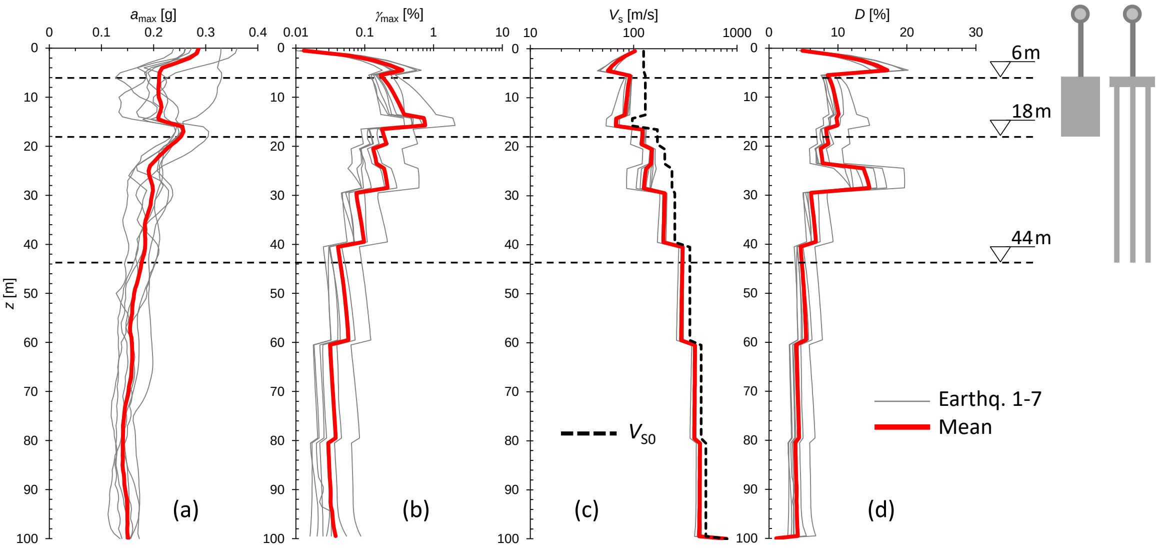

Figure 6. Seismic site response analyses: profiles of (a) maximum acceleration and (b) maximum shear strain, together with the maximum mobilised (c) shear wave velocity and (d) damping.

The results show a concentration of shear strains in the range of 14-16m depth, in correspondence with the peat layer (cfr. Table 1). The presence of the soft peat reduces locally the acceleration, from an approximate value of 0.3 g to 0.2 g, while the average acceleration increases again up to 0.28 g in the shallower layers (0-5m).

A further representation of the results from 1D wave propagation analyses is reported in Figure 7, showing: (a) the transfer function between surface and outcrop accelerations and (b) the elastic response spectra at 5 % damping of the free-field surface accelerations. Moreover, Figure 7b reports the target spectrum for a soil class D, in accordance with the Italian Building Code (NTC, 2018). The mobilization of non-linear soil properties, during the applied earthquakes, reduces the fundamental frequency of the soil deposit from the value of 1.0 Hz to an average value of 0.7 Hz (Figure 7a). Finally, by inspection of Figure 7b it can be noted that the average spectrum inferred from site response analyses (red line) is significantly lower than the corresponding target one (black dashed line), up to periods of about 1s.

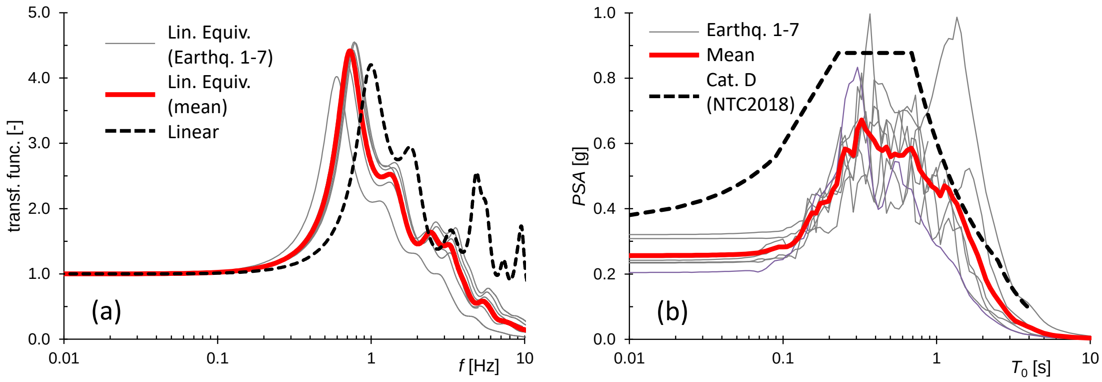

Figure 7. Seismic site response analyses: (a) top to bedrock transfer function and (b) 5% elastic response spectra of surface accelerations.

4 DYNAMIC SSI

4.1 *Numerical model*

The FE model for the shaft was implemented with reference to visco-elastic behavior of the materials, using 2D 4-noded axisymmetric elements. Element height and model width were established ensuring accuracy of the free-field response from comparison to the ground response analysis. The pile group was modelled in 3D, using 8-noded elements.

All the analyses were carried out in the frequency domain, the materials being characterized by a complex Young's modulus. FFT and IFFT algorithms were implemented to switch from frequency to time domain and vice versa.

4.2 *Discussion of results*

The dynamic response of the pier-foundation systems is shown in Figure 8 in terms of non-dimensional steady-state transfer functions, computed in the frequency domain, relating the deck and foundation motion to the free-field motion at surface (U_{ff0}). Specifically, Figures 7 (a) and (b) refer to the shaft and pile foundation, respectively. Regarding the notation, U_{str} is the horizontal displacement at the top of the pier, U_{fnd} is the horizontal displacement of the foundation and Θ_{fnd} is the foundation rotation. Finally, continuous lines refer to Model A (full dynamic SSI), dashed lines refer to Model B (kinematic interaction only), and dotted lines refer Model C (fixed-base structure).

The fundamental frequency of the fixed-base pier, at which the corresponding transfer function reaches its maximum, is $f_{0,\mathrm{FIX}}$ = 1.92 Hz. As expected, dynamic SSI induces an increase of both the deformability ($f_{0,\mathrm{SSI}} < f_{0,\mathrm{FIX}}$) and damping ($\xi_{\mathrm{SSI}} > \xi_{\mathrm{FIX}}$) of the system, the latter being in inverse proportion to the maximum of the $U_{\mathrm{str}}/U_{\mathrm{ff0}}$ curves. On the one hand, the increase in compliance is more evident in the shaft foundation ($f_{0,\mathrm{SSI}}$ = 1.15 Hz), with respect to the pile foundation ($f_{0,\mathrm{SSI}}$ = 1.30 Hz), suggesting that inertial effects are more pronounced in the former case. On the other hand, the reduction in the structural response is more evident in the case of the pile foundation, characterized by a lower peak in the transfer function. This may be interpreted as a higher capability of the piled foundation to increase the damping of the SSI system.

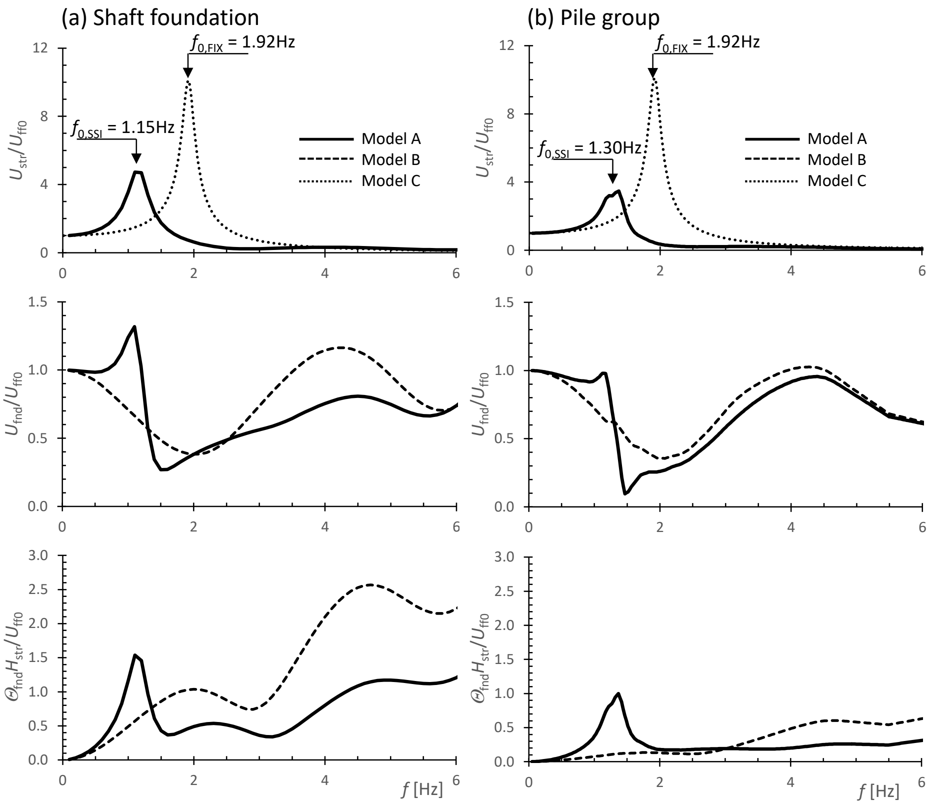

Figure 8. Harmonic steady-state transfer functions between the pier/foundation motion and the free field motion at surface: (a) shaft foundation and (b) pile foundation.

A further insight into the problem can be obtained by looking at the dynamic response of the foundation, affected by both inertial and kinematic effects. As shown in Figure 7, the interaction with the pier is concentrated around the fundamental frequencies of the structure ($f_{0,FIX}$ and $f_{0,SSI}$), where the rotation is maximum, while continuous and dashed lines tend to converge at higher frequencies, where kinematic effects dominate. Consistently with theoretical and numerical observations, the kinematic interaction between the piles and the soil strongly reduces the horizontal motion of the foundation, with respect to the free-field one, without introducing significant rotation (Di Laora & de Sanctis, 2013). On the other hand, kinematic effects still reduce the horizontal motion in the shaft foundation, but a significant rotation emerges in this case (Conti *et al.*, 2017, 2018). This may explains the larger peak in the transfer function of the bridge pier on the shaft foundation compared with that of the pile-supported structure.

A synthetic representation of the time domain response of the structure, under the selected design earthquakes, is given in Figure 9, showing: (a) the maximum absolute acceleration and (b) the maximum relative displacement at the top of the pier, given by the sum of the flexural displacement of the pier and the deflection caused by the foundation rotation. Specifically, the results obtained taking into account SSI effects (Model A) are reported against the corresponding fixed-base results (Model C).

Both foundations reduce the absolute acceleration transmitted to the pier, with an average reduction of 24 % and 41 % for the shaft and the pile foundation respectively. This result was partly anticipated by comparing the elastic response spectra of the free field surface accelerations (Figure 7b) with the fundamental frequencies $f_{0,FIX}$ and $f_{0,SSI}$, which appear in the descending branch of the average spectrum. As previously observed, radiation damping and kinematic interaction participate in reducing further the inertial forces in the structure, even though their individual contribution cannot be isolated by looking at Figure 9.

On the other hand, the horizontal relative displacement of the deck is given by two contributions: (1) the inflection of the pier, induced by the inertial forces in the structure, and (2) the rigid rotation of the foundation, related to the deformability of the soil-foundation system. As already observed, SSI effects reduce the inertial forces but increase the foundation rotation. As a result, the final displacement of the deck strictly depends on the relative importance of these two contributions. Specifically, an increase of 80 % and 14 %, with respect to the fixed-bae model, was computed for the shaft and the pile foundation, respectively.

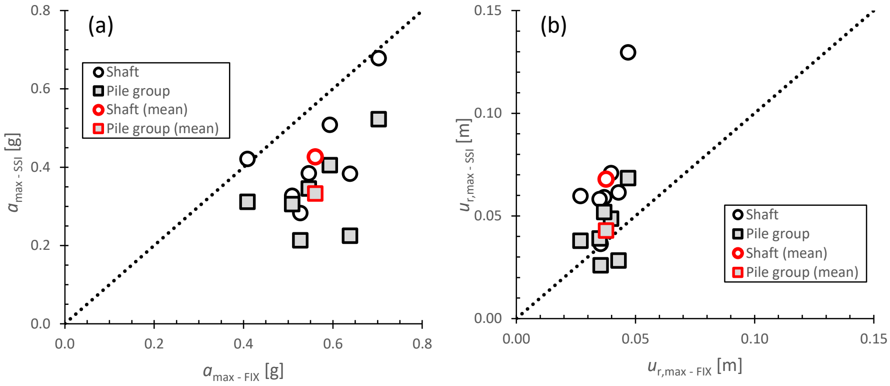

Figure 9. Deck motion under the applied earthquakes: SSI against fixed-base model response. (a) maximum absolute acceleration and (b) maximum relative displacement.

5 CONCLUSIONS

In this work the influence of the type and layout of foundation on the seismic response of a bridge pier on a soft clayey soil has been examined. Reference was made to either a circular shaft foundation or a square (3x3) pile group, both defined in order to satisfy the requirements of the national code for ultimate limit state criteria. The results in the frequency domain show that the reduction of the natural frequency of the fixed base structure induced by the shaft foundation is comparable to that related to the pile group (39% vs 32%). By contrast, while for the pile group kinematic interaction strongly reduces the horizontal motion of the foundation, with no significant kinematic rotation, for the shaft foundation the kinematic rotation leads to an increase of the structural demand in the bridge pier. If the attention is shifted to the time domain, for both foundations SSI effects lead to a reduction of the seismic demand in terms of spectral acceleration, but an increase in terms of bridge deflection. Overall, for the case at hand the pile group resulted to be more efficient in reducing the overall seismic demand in the structure, owing to the higher effective damping.

REFERENCES

Conti R., Morigi M., Viggiani G.M.B. 2017. Filtering effect induced by rigid massless embedded foundations. *Bull Earthquake Eng*., 15(3), 1019-1035.

Conti R., Morigi M., Rovithis E., Theodoulidis N., Karakostas C. 2018. Filtering action of embedded massive foundations: New analytical expressions and evidence from two instrumented buildings. *Earthquake. Engng. Struct. Dyn*., 47(5), 1229-1249.

Darendeli M.B. 2001. Development of a new family of normalized modulus reduction and material damping curves. Ph.D. thesis, Univ. of Texas, Austin, TX.

Di Laora R., de Sanctis L. 2013. Piles-induced filtering effect on the foundation input motion. *Soil Dyn Earthquake Eng.*, 46, 52-63.

Di Laora R., Grossi Y., de Sanctis L., Viggiani, G. 2017. An analytical solution for the rotational component of the Foundation Input Motion induced by a pile group. *Soil Dyn Earth. Eng.*, 97, 424-438.

Iervolino I., Galasso C., Cosenza E. 2010. REXEL: computer aided record selection for code-based seismic structural analysis. *Bull Earthquake Eng*, 8, 339-362.

Mylonakis G., Gazetas G. 2000. Seismic soil-structure interaction: beneficial or detrimental? *J Earthq Eng*., 4(3), 277-301.